BTA/GE/14-16 **An X-ray tomographic investigation into the effects of compressive shear on analogues to charred seeds embedded in archaeological sand**

July 2014 **D.J. Kunst**

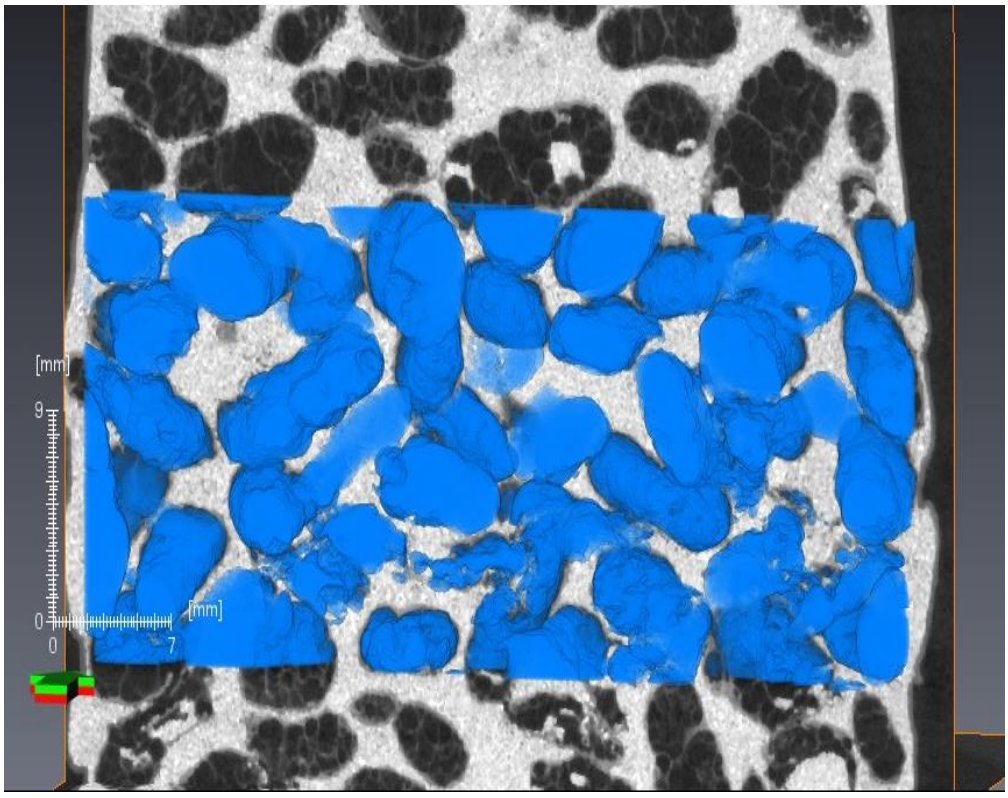

TU Delft Delft University of Technology

Challenge the future

Title	:	An X-ray tomographic investigation into the effects of compressive shear on analogues to charred seeds embedded in archaeological sand
Author(s)	:	D.J. Kunst
Date	:	July 2014
Professor(s)	:	Dr. ir. D.J.M. Ngan-Tillard
Supervisor(s)	:	Dr. ir. D.J.M. Ngan-Tillard
TA Report number	:	BTA/GE/14-16

Postal Address : Geo-Engineering Section
Department of Geoscience & Engineering
Delft University of Technology
P.O. Box 5028
The Netherlands

Telephone : (31) 15 2781328 (secretary)
Telefax : (31) 15 2781189

Abstract

By signing the Valletta Treaty, several countries have obliged themselves to save archaeological heritage sites and fund relevant research. UNDERSTRESS is a proposal for funding which does research and provides data to predict damage done to such archaeological site by construction of linear infrastructure. As a preliminary study this BSc thesis is carried out in the framework of UNDERSTRESS. Although research has been done on archaeological artefacts embedded in sand, charred organic seeds have not been investigated thoroughly yet. The sand, which comes from a depot near Dronten in the Netherlands, has been used because multiple archaeological artefacts have been found in that sand layer. As analogue for the charred organic seeds coco pops, the cereal, have been used. The characteristics of the sand as well as of the coco pops have been investigated. A falling height of fifty centimetres has proven to create a reproducible density. To test the damage to the coco pops samples have been triaxial tested with a vacuum pressure applied of 80 kPA. This vacuum pressure create an effective confining pressure of 80 kPA as well. With the falling height and the confining pressure, a sample configuration in which two layers of coco pops are placed, the damage to those coco pops is zero when applied to a strain of five millimetres. The damage is made visible by using 3D visualising software called Avizo. The grain have not been damage during that test and they have not reallocated as well. For another configuration the coco pops did not react the same. The entire sample was filled with coco pops and sand as supporting material and this time the strain was 15 millimetres. Three scans made at three different times during the loading show that the coco pops are not damaged until after the sample has reached its maximum stress. All the damage to the coco pops as well as the reallocation of the coco pops happens between the peak stress and the unloading. At the slice where the radial deformation of the sample is the largest are all coco pops are damaged with most of them crushed. Two centimetres above and below this slice, the coco pops are partially damage and further away from this slice, the coco pops are not damaged. In total, 10 percent is damaged during the loading. The coco pops are damaged so severely, not much information they have stored would be available if it were charred organic seeds. The charred organic seeds do have twice the strength of a coco pop according to earlier research.

Inhoud

1. Introduction

1.1 Background

When linear infrastructure is constructed on top of soft soils, it leaves its mark in de subsurface. If archaeological sites or artefacts are buried underneath linear infrastructure under construction, they will be influenced as well. In 1992, several countries in Europe signed the Valletta Treaty, also known as Malta convention, to save the archaeological heritage sites. By signing the treaty, the countries are obliged to invest in saving archaeological heritage sites and fund relevant research (Council of Europe, 1992). UNDERSTRESS is a proposal submitted for fund to the Heritage Joint Plus Joint call and the aim of UNDERSTRESS is to do research and provide data to predict the damage done to archaeological remains by the construction of linear infrastructure. This will lead to better and more focussed protection of buried archaeology. This BSc thesis is a preliminary study carried out in the framework of UNDERSTRESS.

There are numerous types of archaeological remains and some are embedded in sand or other sediments. Hyde (2010) has already investigated the resistance of ceramic, glass and bronze artefacts embedded in sand to compressive shear stresses. This investigation will focus on one of the most vulnerable archaeological artefacts recovered in archaeological excavations: the charred organic seeds. It will not use real archaeological remains but analogues to them that are as crushable and weak. Charred organic matter embedded in soils is very resistant to chemical degradation. Charred organic seeds can provide the archaeologists with multiple insights on how former settlements produced food or fed themselves. Charred organic seeds can also provide archaeologists with information about the type of vegetation that was growing in the past and give indications about past climates. Construction works must not endanger the valuable information stored in these artefacts. Van Van Dijk (2014) and Getrouw (2014) did some research on the damage of charred organic seeds when subjected to one dimensional compression. Their combined work show that embedment of crushable particles in sand has a beneficial effect on their resistance to one dimensional loading. Getrouw (2014) showed that the breakfast cereal coco pops could be used as analogues to charred organic seeds by comparing their individual crushing strength.

In this thesis, focus is to put on the resistance of crushable particles embedded in sand to compressive shear stresses. Shear stresses are more destructive than one dimensional compression. While one-dimensional stress-strain conditions prevail under the central part of the embankment, shear stresses prevail at the toe of the embankment. They are also generated during construction work like pile driving.

This thesis will contribute to provide archaeologists with a decision making tool on preserving the charred organic seeds. This decision making tool will consist of a probability range on the degree of integrity to the applied stresses.

1.2 Objectives

To get to the actual investigation and the probability range, multiple objectives have been set.

1. Determine the index properties of the sand used in the experiments.

2. Create sand samples with the a known density and reproducible mixtures of sand and artefacts with a given artefacts to sand ratio.

3. Quantify the damage sustained by artefacts that have been manually seeded in sand and have been subjected to triaxial shear compression. To reach this goal, select a configuration which is likely to generate damage.

1.3 Methodology and report structure

To fulfil the first objective, it is necessary to get familiar with the equipment used for traditional soil sample classification tests such as dry sieving, pycnometer testing, minimum and maximum void ratio determination. The results are presented in chapter 2.

To fulfil the second objective, first, literature is reviewed and a preparation method of which others have proved it works, is adopted to produce sand samples of a given density. This is explained in chapter 3.1. Second, a trial and error procedure is used to seed the sand with particles that are analogues to crushable charred organic seeds is used. This is explained in the rest of chapter 3.

To fulfil the third objective, simplified triaxial tests are conducted so that X-ray micro-computed tomography can be used to quantify the integrity of the inclusions without having to build a triaxial cell transparent to X-rays. The scans are realised at different stages of the test. This will be explained in chapter 4 & 5 while the results will be discussed in chapter 6. In chapter 7 the conclusions are drawn and recommendations are made in chapter 8.

2. Materials

2.1 Sand

The sand being used for these test is a Pleistocene cover sand recovered from the subsurface underneath the “Prorail depot” at Dronten, the Netherlands. This sand has been retrieved after construction of the depot from the continuous Begemann borehole D9. In this cover sand layer, multiple archaeological artefacts of the Neolithic age have been found.

After transportation to the laboratory, the linings of borehole D9 have been opened and cut into halves longitudinally for description. The two halves of an interval of one meter containing Pleistocene sand have been selected for this research. Before construction, this interval was around five meters below the original ground surface. Now it is seven m below the man-made ground surface

2.1.1 Grain size distribution

To avoid segregation during preparation of the sand and artefacts mixtures and perturbation of the micro-CT image processing by impurities in the sand, only sand with a particle diameter between 63 and 250 µm is used in this investigation. Figure 1 presents the grain size distribution of two samples of this "clean" sand.

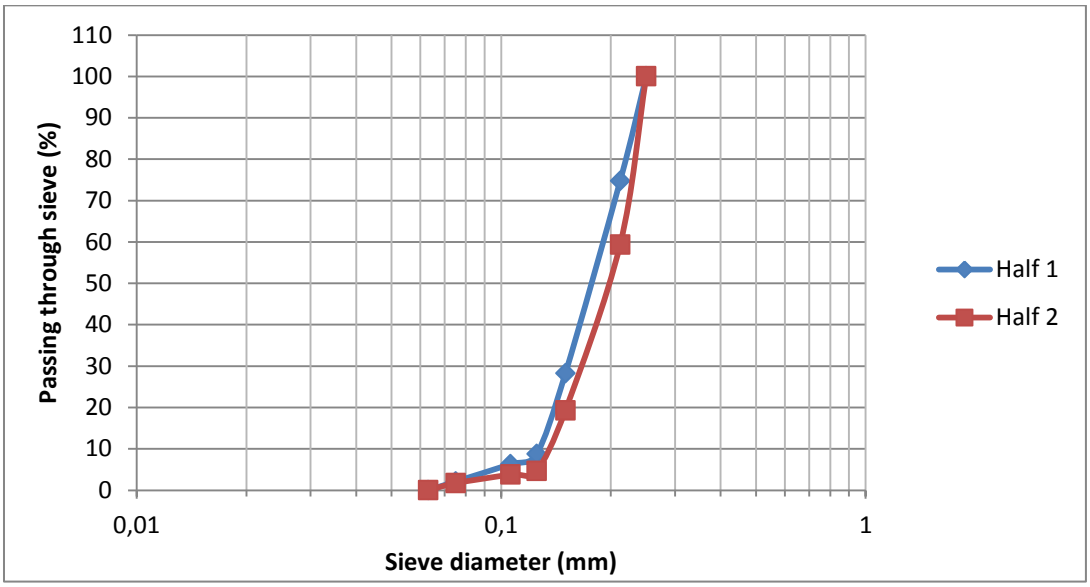

Figure 1 Sieve curve for sand from Dronten Prorail depot.

These two curves look almost the same. In soil mechanics, characteristic particle diameters called D_x are derived from a grain size distribution curve, with x….: D_{10}, D_{30}, D_{50}, and D_{60}. D_{50} is used to indicate the coarseness of the sand. With an average D_{50} of 0.190 mm (Table 1 Sieve curve indication of both intervals), the sand is categorized as moderately fine. D_{10} , D_{30}, and D_{60} are used to calculate the coefficients of uniformity and curvature of the sand and classify the sand in terms of grading. The coefficient of uniformity can be calculated by:

$$Cu = \frac{D_{60}}{D_{10}}$$

The coefficient of curvature can be calculated by:

$$Cc = \frac{{D_{30}}^2}{D_{10} \cdot D_{60}}$$

With an average Cu of 1.55 and an average Cc of 0.965 (Table 1 Sieve curve indication of both intervals the sand is classified as very uniformly graded or in other words, very poorly graded.

	Half 1	Half 2
D10	0,127	0,135
D30	0,153	0,167
D50	0,18	0,198
D60	0,193	0,213
Cu	1,52	1,58
Cc	0,96	0,97

Table 1 Sieve curve indication of both intervals

2.1.2 Void Ratio

The more space there is within the sample, the more space there is for deformation of the grains and therefore more deformation for the entire sample. The space between grains influences both the volumetric behaviour and peak strength of the sample (Wood, 2008). The void ratio (e) is the ratio of the volume of the voids and the volume of the solids and it is related to the porosity (n) that is more commonly used in geoscience as follows:

$$e = \frac{n}{1-n}$$

The porosity can be calculated by using the density of a grain, γ_s, and by using the dry density of the sample as follows:

$$n = 1 - \frac{\gamma_d}{\gamma_s}$$

The density of a grain has been determined using a gas pycnometer. It corresponds to the density of quartz grains (Table 2).

The actual void ratio of a sample is compared to the minimum and maximum void ratios (e_{min} and e_{max}) that can be obtained by calculating the relative density (RD).

$$RD = \frac{e_{max} - e}{e_{max} - e_{min}} \cdot 100\%$$

A sample with a relative density between 35% and 65% is said to be medium dense.

Several methods have been proposed to determine these minimum and maximum void ratios. In this research, both ratios are determined with the Japanese method (Anaraki, 2008). For the maximum void ratio, the sample has been built by pluviating sand in a mould with a falling height of 50 millimetres. The weight of the sample can be measured on a scale and the volume of the mould can be calculated, so the density can be determined. For the minimum void ratio, the sample has been built in five layers. After each layer, the mould has been tapped a hundred times. Again, the weight can be measured and the volume is now known so the density can be calculated.
The maximum and minimum void ratio are displayed in Table 2.

Specific Gravity [-]	Max Void Ratio [-]	Min Void Ratio [-]
2,65	0,81	0,48

Table 2 Specific gravity, maximum and minimum void ratio of the sand

2.2 Coco pops

Due to limited resources of real archaeological charred seeds, an alternative had to be found to replicate the charred seeds. Coco pops, a breakfast cereal, seems to be a good analogue. They have the same size and shape, they present and inner porosity and, according to Getrouw (2014), they also have the same resistance and progressive failure pattern as vulnerable wheat seeds carbonized at 370°C. These Coco pops will be used to do the first round of testing not to waste any real archaeological charred seeds on trial runs. We could also have chosen to prepare our own charred grains but it would cost too much time to obtain the material of the right strength in sufficient quantity ((Van der Putte, 2011).

The dimensions of the coco pops are useful for calculating the actual density of the sand present in a sand sample seeded with coco pops. The volume is calculated assumed the coco pops are ellipsoidal. Average values are listed in Table 3.

	Axis (mm)			Volume (cm^3)
	Longest	Shortest	Middle	
1	11,7	3,8	7,4	1,37
2	10,55	4,2	6,3	1,17
3	10,8	4,4	6,2	1,23
4	12,65	3,4	6,8	1,23
5	10,05	3,85	6,6	1,07
Average	11,15	3,93	6,66	**1,22**

Table 3 Coco pop measurements and average

The behaviour of the individual coco pop and peak strength during individual crushing tests have been derived from Getrouw (2014). See Figure 2 and Table 4.

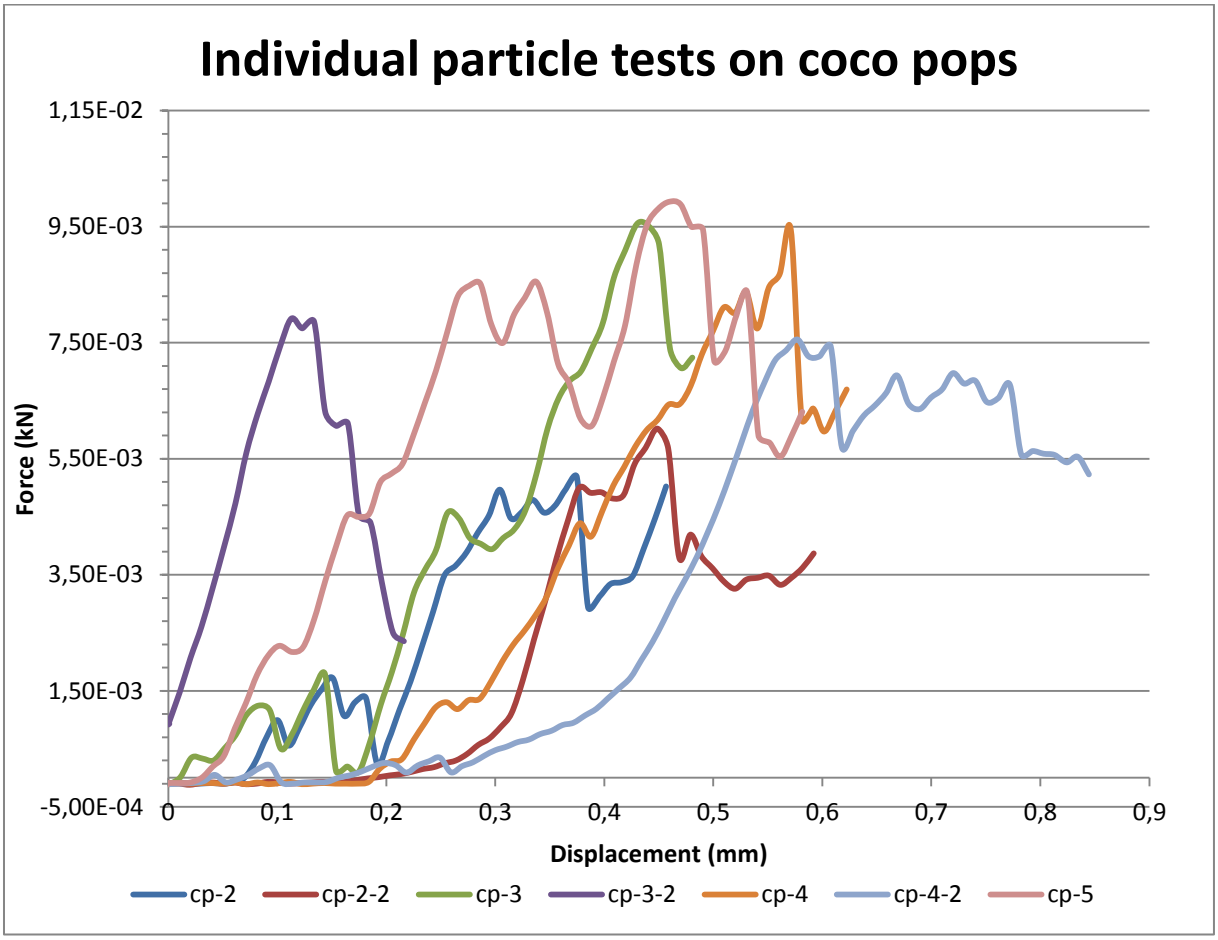

Figure 2 Force against displacement of individual coco pops, data acquired by Getrouw (2014).

	Max Force (kN)
cp-2	5,18E-03
cp-2-2	6,02E-03
cp-3	9,55E-03
cp-3-2	7,92E-03
cp-4	9,45E-03
cp-4-2	7,56E-03
cp-5	9,93E-03

Table 4 Peak strength of different coco pops. When after unloading a particle was not clearly splitted into two or more fragments, it was re-loaded again to failure.

Failure is progressive as some part of the coco pop gets crushed or inner void collapses and load is transferred to the remaining part of the coco pop. The peak force of the coco pops ranges from 5 to 10 Newtons. By similarity to Brazilian tensile strength tests on disks, their tensile strength can be estimated by dividing the peak force by the square of distance between the loading plates, assumed here to be the average shortest axis of the coco pops. Tensile strength values are indicated in Table 5. They are much lower than the tensile strength values of the artefacts tested by Hyde (2010).The weakest artefacts tested by Hyde were calcareous ceramics fired at 750^{o}C with a tensile strength of 8 MPa.

	Tensile Strength (kPa)
cp-2	335
cp-2-2	390
cp-3	618
cp-3-2	513
cp-4	612
cp-4-2	489
cp-5	643

Table 5 Tensile strength of the coco pops

Besides the peak strength, the minimum and maximum void ratio of the coco pops has been determined as well. When using the Japanese method in the same way as with the sand, the void ratio can be determined (Table 6).

Specific Gravity [-]	**Max Void Ratio [-]**	**Min Void Ratio [-]**
1,21	6,76	6,09

Table 6 Specific gravity, maximum and minimum void ratio of the coco pops

No particle crushing was observed during the tapping of the mould.

3. Sample Preparation

3.1 Dry air pluviation

To create the sample, the dry sand pluviation method was used as explained by Van Nes (2004). The falling height of the sand, when using the dry sand pluviation method, determines the density of the sample. The higher the falling height, the higher density. In this method, the sand is stored in a funnel with a long stem. The long stem is to distribute the sand accurately over the total diameter of the sample as well as to avoid air turbulence. The sand falling through the funnel is being captured by the sample container below a certain distance to the funnel. The falling height is being measured with a ruler that has been placed next to the sample container. In order to create a sample with a homogenous density, the falling height has to remain constant. Therefore, the funnel will have to be raised gradually accordingly to the increasing height of the sample. The funnel is also circled within the boundaries of the sample to distribute the sample equally and create the homogenous sample needed. In Figure 3, a schematic picture can be seen of the setup.

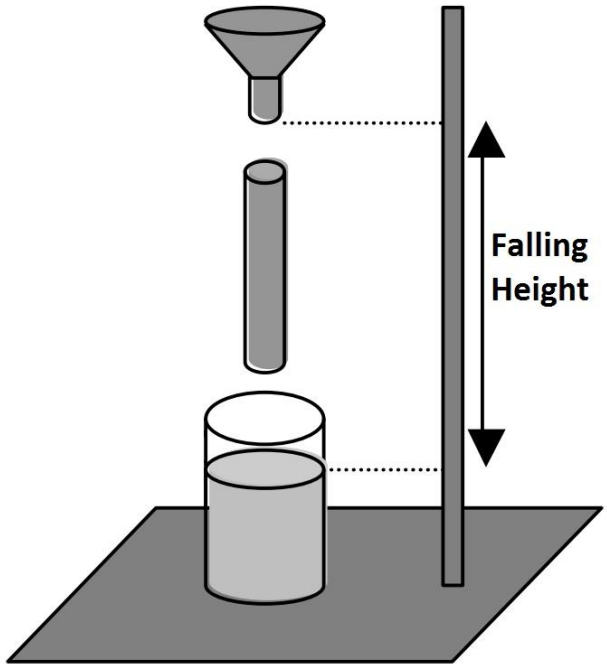

Figure 3 Setup to create sand sample with dry pluviation (Van Nes, 2004).

3.2 Density – falling height relation

The sand sample density is related to the falling height according to Stuit (1995). In order to establish this relationship for the sand used for testing, multiple samples had to be made at different falling heights and their density has to be measured (Table 7 & Figure 4).

Falling Height (mm)	Test Number	Sample weight (g)	Volume (cm^3)	Density (g/cm^3)
27,67	1	311,95	215,98	**1,44**
	2	305,27	210,73	**1,45**
	3	314,96	211,31	**1,49**
	4	313,38	211,79	**1,48**
37,67	1	323,67	209,95	**1,54**
	2	314,14	210,15	**1,50**
20,67	1	304,64	206,28	**1,48**
	2	304,37	208,02	**1,46**
	3	306,61	211,60	**1,45**
	4	312,62	209,37	**1,49**
	5	308,2	208,21	**1,48**
30,67	1	320,74	211,02	**1,52**
	2	322,03	212,08	**1,52**
	3	311,54	211,89	**1,47**
	4	316,16	212,18	**1,49**
40,67	1	325,32	213,04	**1,53**
	2	320,87	210,15	**1,53**
	3	330,19	213,53	**1,55**
	4	325,4	213,62	**1,523**
	5	330,93	211,40	**1,57**
50,67	1	330,91	210,53	**1,57**
	2	334,81	212,47	**1,58**
	3	335,18	212,18	**1,58**
	4	331,64	213,14	**1,56**

Table 7 Falling Height - Density Relationship

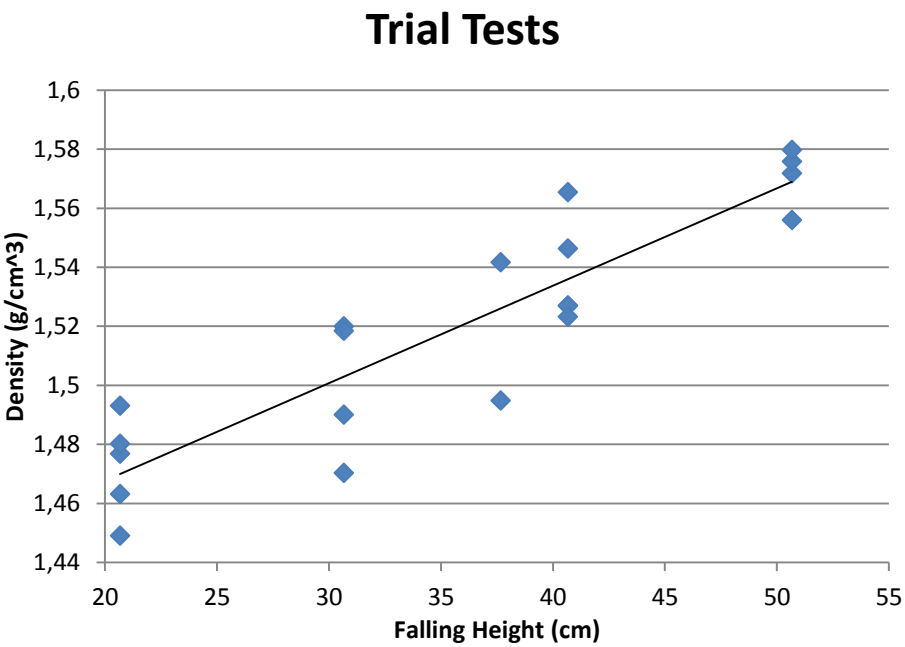

Figure 4 Trial test on the density vs. the falling height

The first two tests, with a falling height of 27 and 37 cm, did not come out accurate due to lack of experience. The lowest density spreading is obtained for the last trial tests done with a falling height of 50 centimetres. This falling height is therefore used to create the samples. Based on the measured minimum and maximum void ratios (section 2.1), the sand samples prepared for triaxial testing have a relative density of 0.355 and are therefore medium dense sand.

3.3 Sample configurations

Multiple samples are made in order to investigate mixtures with various fractions of coco pops. The first sample is made by sand pluviation and approximately every two centimetres, the sand flow is stopped using the plug. A layer of coco pops is added on top of the sand with the longest axis of the coco pops horizontally (Figure 5 & Figure 6). This arrangement of coco pops is thought to resemble the real arrangement of archaeological carbonized seeds in sand. This point should be checked with archaeologists.

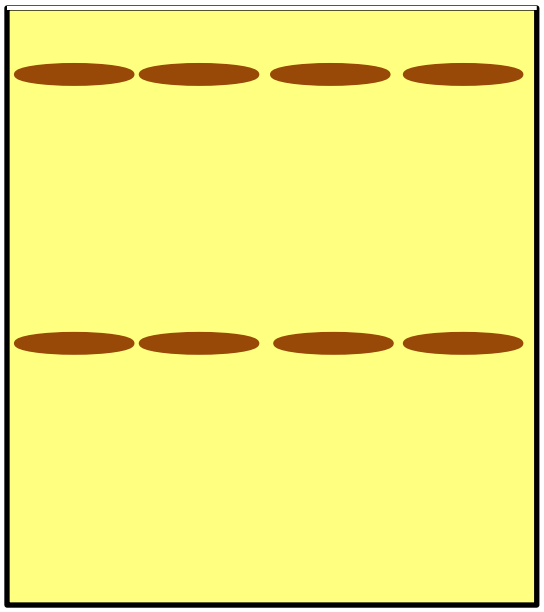

Figure 5 Side view of coco pop layer in the sample

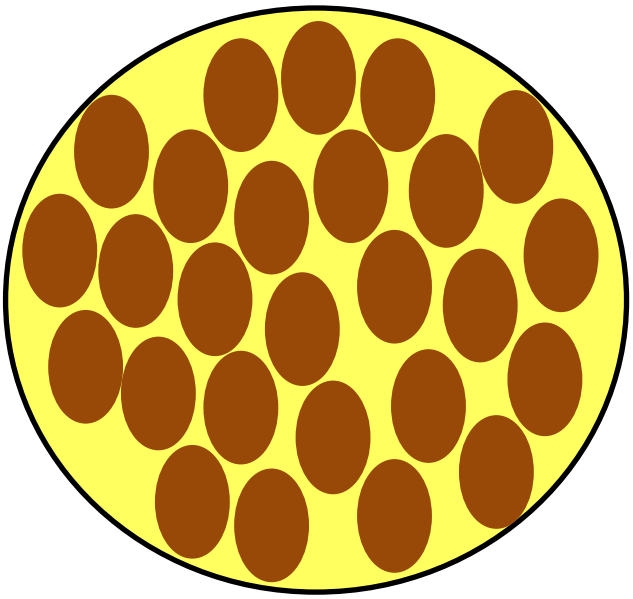

Figure 6 Top view of coco pop layer in the sample

The second configuration that is used is a configuration in which the majority of the sample consists of coco pops contrary to sample one which consists mostly of sand.

The coco pops are poured into the mould until approximately two centimetres have been added. Then, the sand is pluviated at the same falling height, 50 cm, as the other samples. The sand pluviation is stopped as soon as most of the voids are filled and just before they cover up the coco pops completely. Again, 2 cm of coco pops are added and sand is pluviated to fill the voids. This cycle is repeated until the entire mould has been filled with coco pops and sand (Figure 7 & Figure 8).

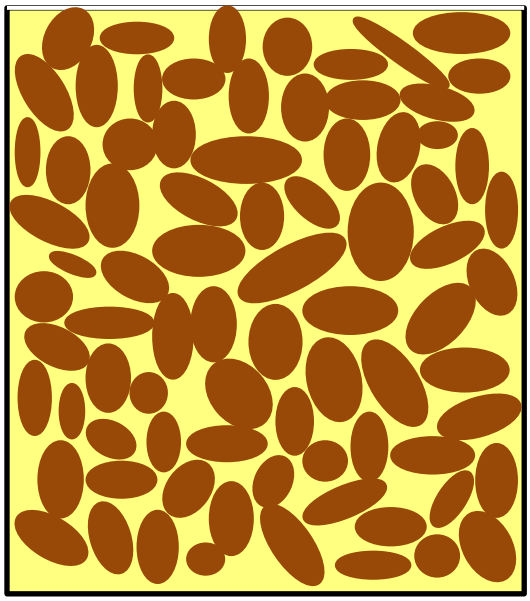

Figure 7 Side view of the second coco pop distribution

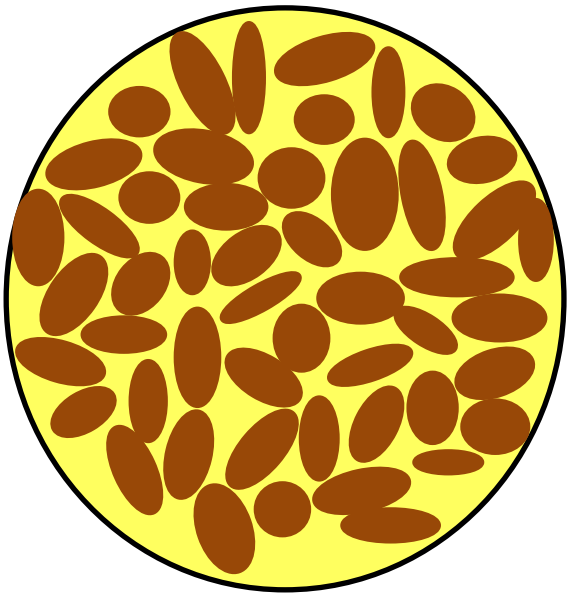

Figure 8 Top view of the second coco pop configuration

3.4 Preparation of sample for triaxial testing

The preparation of samples by dry pluviation for triaxial testing is done following the procedure described below. The following objects are needed for making the sample so that it can be transported and positioned on a compressive loading frame:

- Bottom and top loading plates
- Latex membrane (0.2 mm thick, 150 mm long)
- Four o-rings
- Ruler
- Calliper
- Split mould (consisting of 3 pieces, together 50 mm inner diameter)
- Split mould ring with slightly larger diameter than split mould
- A funnel
- A plug

Step 1: The latex membrane is placed around the bottom plate and secured with two o-rings in order to seal the membrane airtight.

Step 2: The split mould is assembled by putting the three pieces next to each other and secure them by a ring with a slightly larger diameter. The assembled mould is placed around the bottom plate with the membrane. A vacuum pressure is applied between the membrane and the mould. The membrane is stretched to line the mould and the top of the membrane is stretched over the mould.

Step 3: The actual sample can now be made using the dry pluviation method. The height at which the top of the funnel needs to start and end is calculated to ensure the same falling height. The length of the stem if included in the falling height. A plug is used to stop the sand from falling already until the entire funnel has been filled. The plug is removed as soon as the top of the funnel is at the right height. The funnel has to be raised and circled to create a homogenous deposition. When the sample container is completely filled, the leftover sand on top is removed with a ruler to create a flat top surface.

Step 4: A top cap is placed on the sand. Holding the cap down by finger pressure, the membrane, that was stretched around the mould, is pulled upwards so it stretched around the top cap. To secure the membrane at the top, two o-rings are placed around the membrane an top cap to create an air sealed sample.

Step 5: The pump is released from the mould and attached to the bottom plate. Once the valve is opened, vacuum is applied to the sand in the container. The ring around the mould is removed and the three mould pieces are removed as well. With the removal of the mould, the sample is ready for the triaxial tests.

4. Triaxial Testing

A triaxial test is used to determine the behaviour of a sample when applied to deviatoric stresses. Several stress paths can be applied. In most cases, the sample is placed in a pressure cell for applying an all-around pressure on the sample and a top plate can be moved vertically in order to apply an additional vertical stresses on the sample. The radial stress (confining pressure) is constant, while the axial stress generated by compressing vertically the sample at constant strain rate increases (Figure 9).

There are three main types of triaxial testing.

- Consolidated – Drained (CD)
- Consolidated – Undrained (CU)
- Unconsolidated – Undrained (UU)

When a triaxial test is consolidated and drained, a first stage of applying confining pressure together with allowing drainage is carried out. After that first stage, the difference between the confining stress and vertical stress, the deviatoric load, is applied. When a test is consolidated and undrained, the first stage of applying confining pressure is carried out but the drainage valves are closed. With an unconsolidated and undrained triaxial test, the deviatoric load is immediately applied and the drainage valves are closed (Geotechdata.info, 2010).

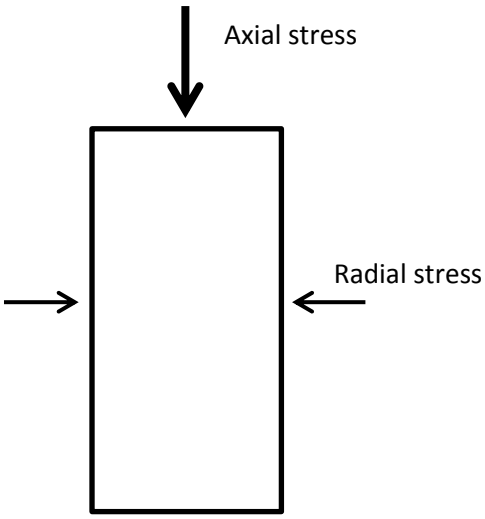

Figure 9 Schematic drawing of axial and radial stresses in triaxial test

In this research, simplified drained triaxial tests are conducted. The sample is maintained at constant effective stress by applying a constant vacuum pressure (-80 kPa) inside the sample. Since the external confining stress is 0 and the pore pressure is equal to the vacuum pressure (-80 kPa), the effective confining stress is 80 kPa. The tests are drained since the vacuum pressure is kept constant.

After the sample has been built, vacuum is applied. When the sample is under vacuum, the valve of the vacuum line is closed and the sample is transferred to the triaxial testing frame. A vacuum pressure is applied again during testing. The compression is carried out using a universal testing machine at a constant displacement rate of 1 mm per minute. Such a high displacement rate can be

applied since the sample is dry and no consolidation phenomenon takes place. It is chosen arbitrarily to use the vacuum pump at this maximum capacity (-80 kPa). Assuming a horizontal to vertical stress of 0.5 for a medium dense sample, an effective confining stress of 80 kPa corresponds to an effective vertical stress of 160kPa, equivalent to 20 m of sand with a submerged density of 8 kN/m^3. Future tests should be done using lower vacuum pressure to simulate pressures prevailing in the Pleistocene cover sands where many Neolithic settlements have been found and investigated in Netherlands.

Effects of confinement on sample purely assembled of coco pops

A sample was made only consisting of coco pops in order to investigate whether significant crushing occurs when vacuum is applied. Four different vacuum pressures were applied: 80, 60, 40 and 20 kPa. The sound of cracking coco pops could be heard during application of the vacuum at all four different pressures. However, when coco pop layers were placed in a sand sample and a vacuum of 80 kPa was applied, there was no sound of coco pops breaking. When the sample was released from the vacuum, the coco pops were examined. All coco pops were found to be intact. The sand supported the coco pops when the vacuum pressure was applied. The pores of the coco pops, however, were not filled with sand. This outcome approves the use of the external volume of coco pops to determine the density of the sand in the sample. The calculated density should be anyway close to that related to a falling height of 50 cm.

5. Micro-CT scan

X-ray Micro-CT (or micro-Computed Tomography) is an imaging technique which provides geometrical information about the inner structure of a sample in three dimensions. Microtomography is based on X-ray radiography and allows the creation of a 3D model of the sample consisting of a set 2D images, without destructing the sample. The resolution of the model is related to the size of the sample. It is about 1/1000th of the sample diameter. In this study, the resolution of model is 0.060 mm. It corresponds to the size of the edge of the voxel, the elementary volume of the model. The true spatial resolution is higher (less good) but has not been determined. The grey level of each voxel of the model represents the X-ray attenuation of the material(s) present in this voxel. The set of 2D images can be processed to filter out noise, calculate the sample porosity, visualise its particles, separate them and quantify their morphology. In this investigation, the scans are made with the Nanotom S manufactured by General Electrics and the scans are processed with AVIZO, a powerful commercial visualising software.

Samples subjected to 80 kPa effective confining pressure are stiff. Transportation to the micro-CT scan while under vacuum is unlikely to damage them. In this investigation, 2 samples have been scanned, both of them at the initial stage before triaxial testing and after large deformation. One sample has also been scanned at about the peak strength. Focus is put on the integrity of the coco pops
as well as on their displacement and rotation. From the high resolution scans, the dimensions of the fragments belonging to the same coco pop can be ideally determined and the degree of integrity of the coco pop can be calculated by dividing the volume of the largest fragments by the initial volume of the coco pop. This definition is similar to that used by Hyde (2010).

Figure 10 The Micro-CT scanner

6. Results

6.1 First test

The first test was done on a sample which contained two coco pop layers. The layers were separated approximately of two centimetres from each other. As already described, two micro-CT scans have been made of the sample, one before the loading and one after the loading with a strain of 5%. The stress versus axial strain recorded during this test is shown in Figure 11. The stress – strain curve tends asymptotically to the value of 0.25 MPa. This value is therefore the maximum stress as well. The sample itself did not deform heavily during testing. The diameter at the centre of the sample did increase, but shear bands stayed away (Figure 12).

With the use of Avizo and a function called “Volume Rendering”, the two coco pop layers have been visualised before the loading (Figure 13 & Figure **14**) as well as after the loading (Figure 15 & Figure 16).

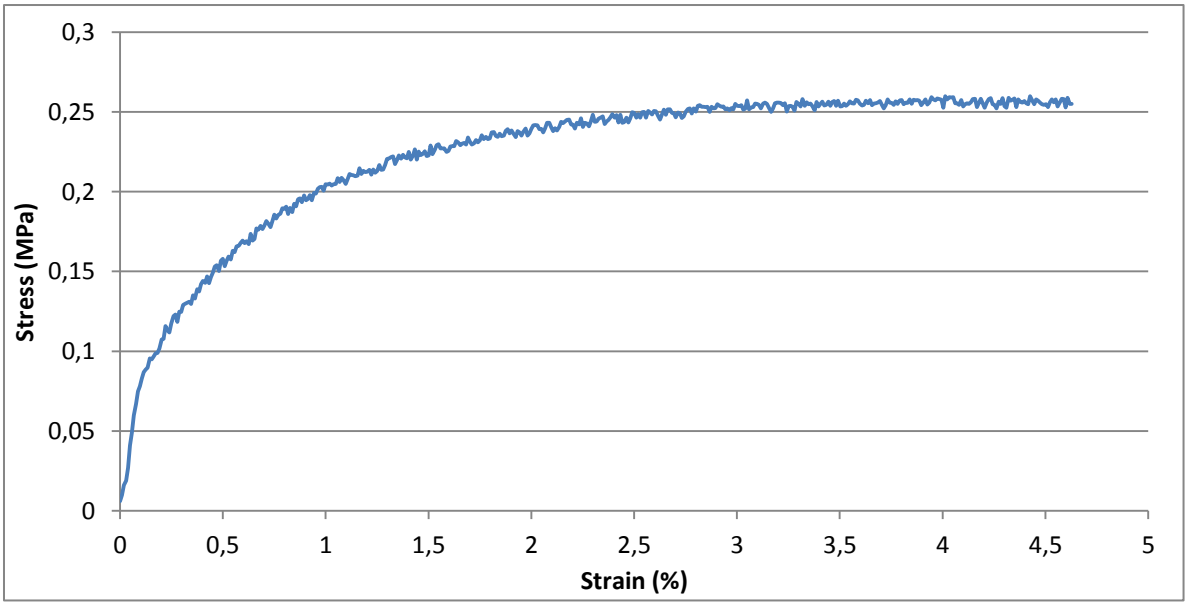

Figure 11 Stress - strain curve for the first sample

Figure 12 First sample in the universal testing machine during loading

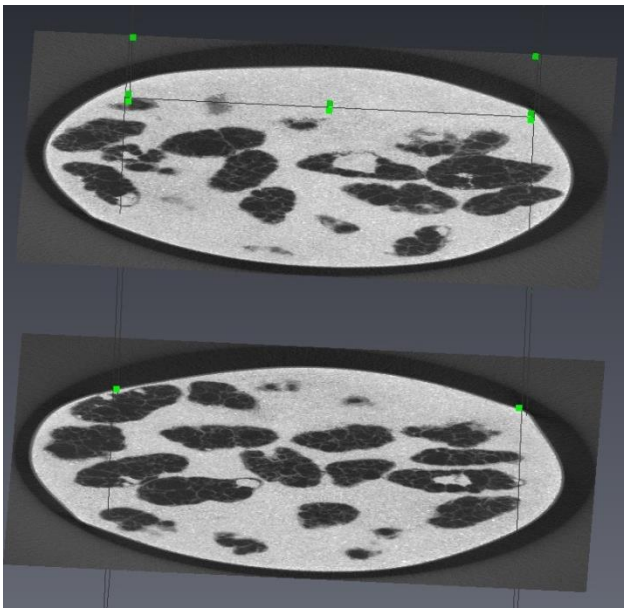

Figure 13 CT images of the two coco pop layers before loading. The scale is given by the sample diameter (55 mm).

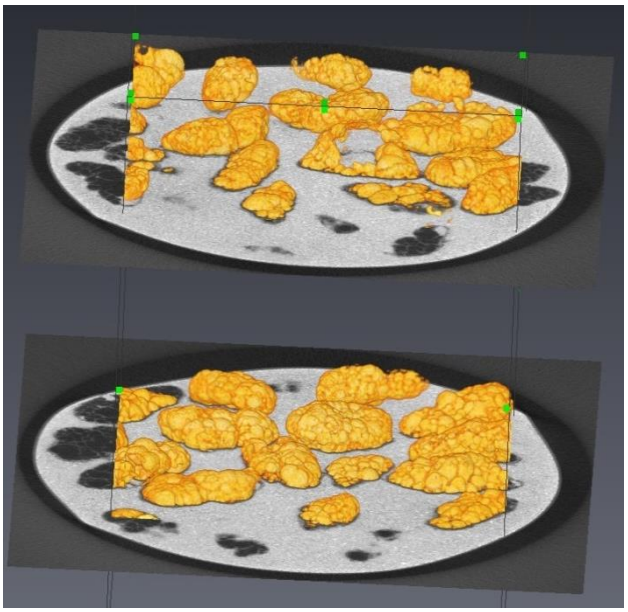

Figure 14 Visualisation of the two coco pop layers before loading. The scale is given by the sample diameter (55 mm).

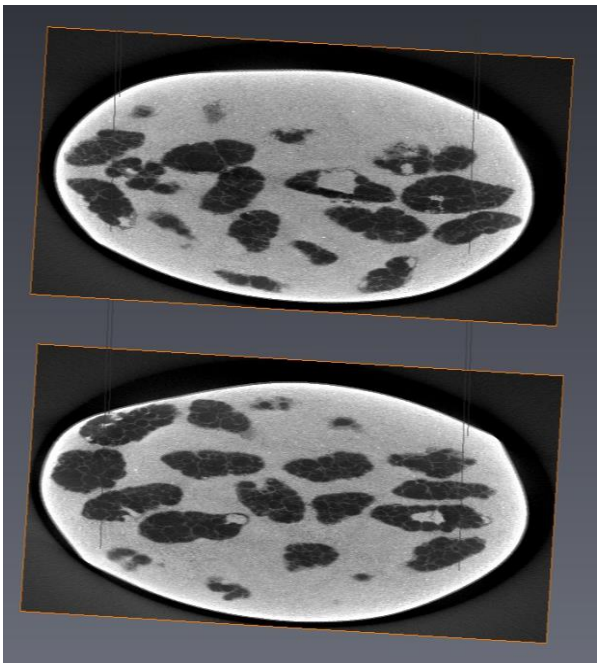

Figure 15 CT image of the two coco pop layers after loading. The scale is given by the sample diameter (55 mm).

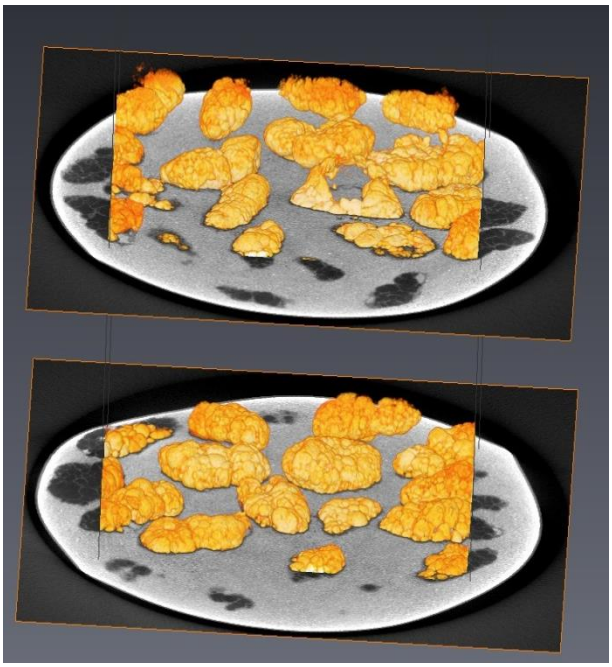

Figure 16 Visualisation of the two coco pop layers after loading. The scale is given by the sample diameter (55 mm).

The volume rendering of the coco pops layers before and after testing allows a clear visualisation of the coco pops (Figure 16 & Figure 17). All coco pops are intact.

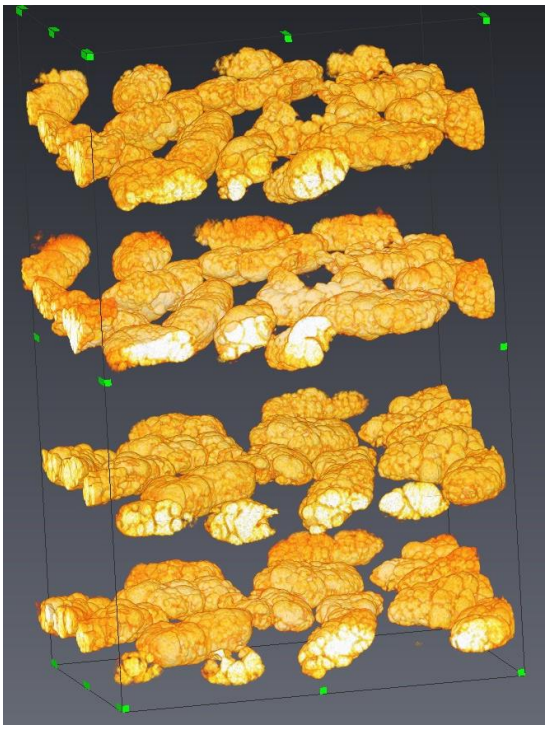

Figure 17 Coco pops layers 1 and 3 (counted from the top) are before loading, 2 and 4 are after loading

As can be seen, the coco pops haven't been moved in any other direction than along the z-axis, nor have they been damaged by the loading. When the sample was opened, no broken coco pops were found in the sample. The strain was diffuse through the whole sample rather than being localised in a shear band. As the test was stopped at a relatively lower axial strain, coco pops did not get crushed.

6.2 Second test

For the second series of tests, the fraction of coco pops was significantly increased. The sample consisted of coco pops with sand used to fill up the voids between them. A first sample was produced and tested in the universal testing machine. The test was terminated at a higher maximum strain than test one. The stress strain curve for this sample is displayed in Figure 18.

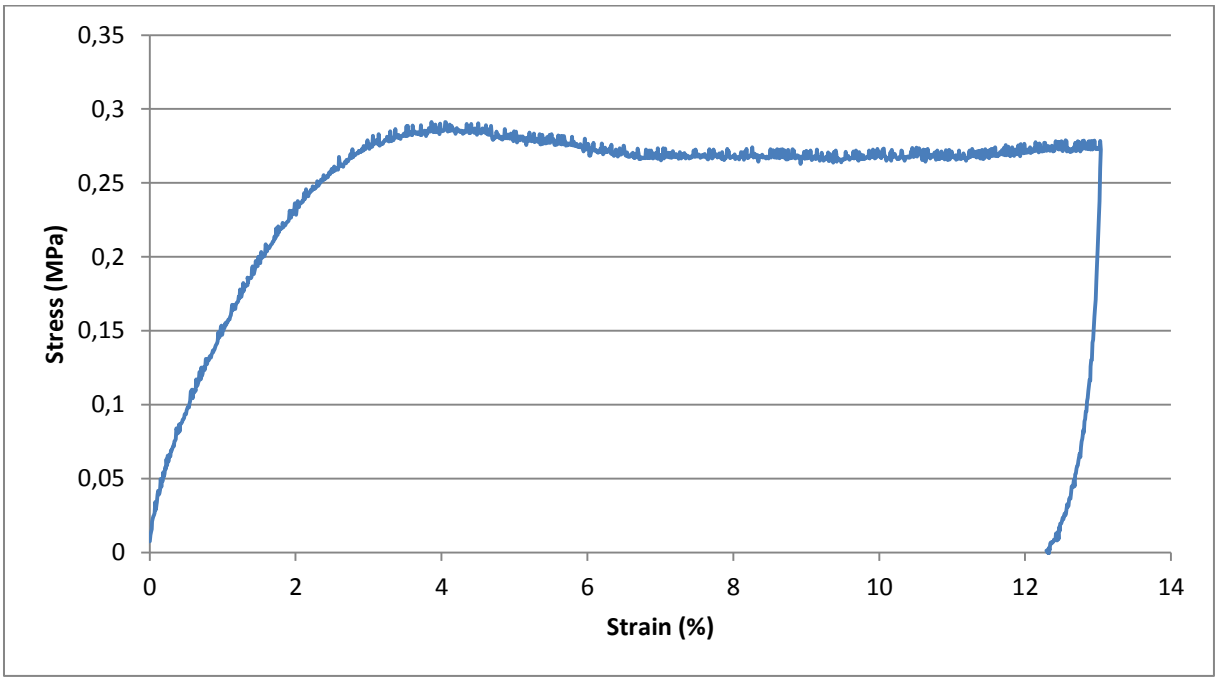

Figure 18 Stress - strain curve of the second test

In this stress – strain curve, a peak is visible that corresponds to a maximum stress value of 0.29 MPa. After the peak, the stress falls back and stays around the same value for the rest of the test. During unloading, the sample has a stiff response.

The sample changed from a cylinder to a barrel. The sample diameter increased significantly in the centre of the sample (from 46 mm to 57 mm at the most) and the sample showed shear band structures on its external surface (Figure 19). The coco pops present in the sample and the penetration of the membrane into the sample make the deformation look strange.

When the sample was opened, multiple coco pops were broken. In order to get a good idea where most of the broken coco pops were found in the sample, the sample has been opened in three parts (Figure 20). For each part of the sample, the coco pops were counted and the number of broken coco pops, completely crushed or partially broken, was written down (Table 8).

Part	Height (mm)	# Coco pops	Crushed	Partially broken	Crushed (%)	Partially broken (%)
1	20	177	0	0	0	0
2	70	367	32	38	8.7	10.4
3	20	182	0	6	0	3.3
Total	110.8	726	32	44	4.4	6.1

Table 8 Counting of the broken coco pops (crushed or partially) for every part of sample 2

Most of the coco pops that are broken were found in the part of the sample where the shear bands are formed.

Figure 19 Second sample after loading

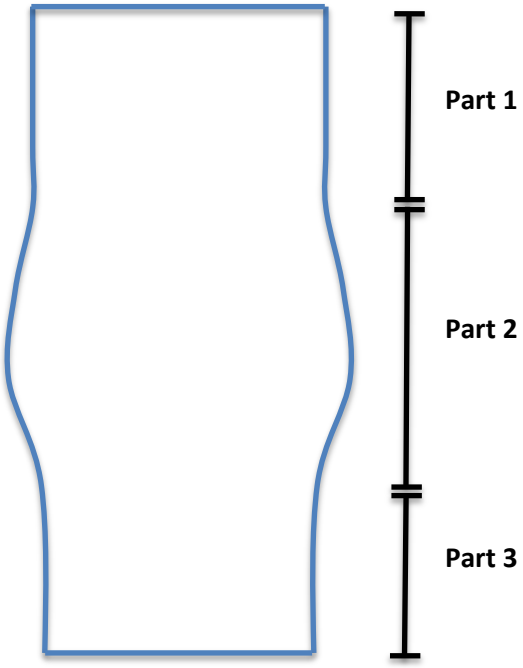

Figure 20 Overview of opening sample 2 in parts

6.3 Third Test

The essence of this test is the same as the previous test. A sample has been made in the same way and the testing was done the same as well. Only this time, the sample has been scanned three times. Once before the testing, once when it was unloaded after having reached its peak stress and once after 13% strain and final unloading (Figure 21).

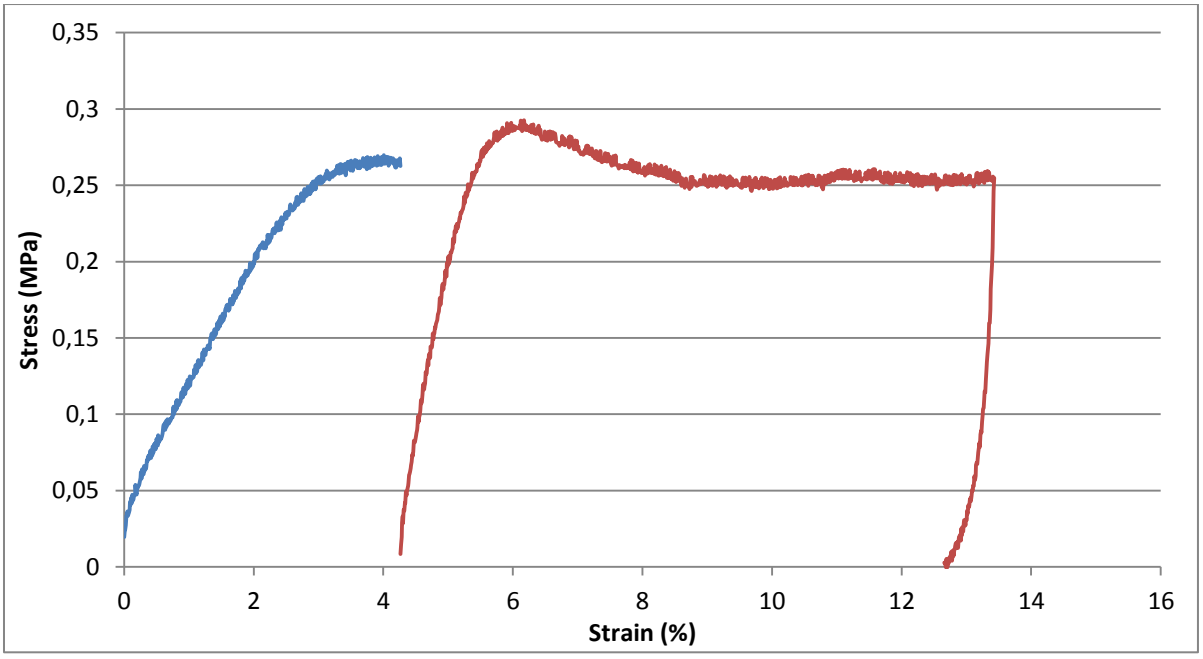

Figure 21 Stress - strain curve for the third sample combined out of two tests. Between the blue and the red curve a second CT-scan has been made of the sample.

About it can be noted that after unloading at peak strength and reloading, the sample is able to reach a higher peak stress than before the unloading. Apart from that, the test looks normal. Moreover, the second peak strength is identical to the one measured in the trial test without scans.

The scans made at three different times during the loading provide information about the time most coco pops get damaged (Figure 22). The sample was too high to be scanned in one scan. Only part of it was scanned. At the last scan, the elevation of the sample on the rotating stage of the scanner was adjusted so that the most deformed part of the sample was entirely scanned. The scans have been cropped so that a volume containing the same grains is analysed at each of the 3 stages of deformation. The cropping is done visually.

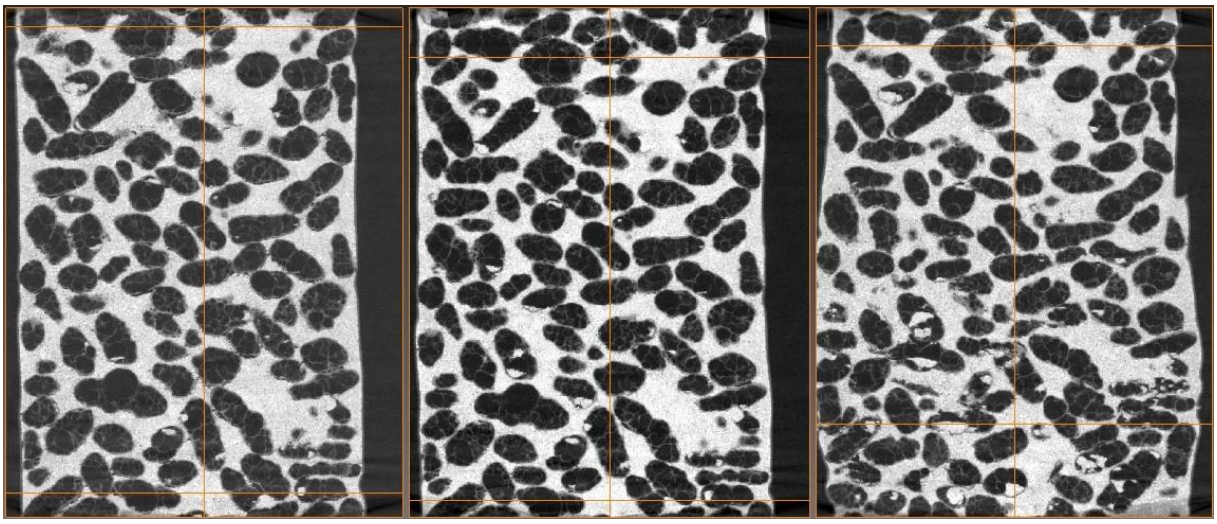

Figure 22 Side view of sample. Before loading, at peak stress and after loading. The thin orange lines on the top and the bottom of all three scan correspond to each other.

Sample deformation and coco pop movements and damage

The main difference between the scan before loading and the scan taken at the peak stress is the vertical shrinking of the sample and the slight increase in the sample diameter. Coco pops have kept the same relative orientation with respect to each other. Very few, if any, coco pops have been damaged yet.

When comparing the scan taken at the peak stress and at 13% strain, the change of shape of the sample is obvious. At 13% strain, the sample has a deformed barrel shape and is cut by shear bands (figure 22, right). Its diameter has increased so much that part of the sample is about to fall outside the scan; the scan being made at the same magnification as the first scan. Moreover, a lot of damage is visible in the coco pops, especially at the bottom of the scanned area (figure 22, right). Multiple coco pops have been crushed or severely damaged and they all are along the same line in the sample where the sample diameter is the largest. Last but not least, coco pops have moved relatively to each other between the peak stress and the 13% strain stage. They are closer to each other than they were at the peak stress.

When zooming at the scans (Figure 23 and Figure 25), the type of displacement, rotation and damage that the coco pops have sustained can be seen clearly. When using AVIZO visualisation possibilities like thresholding and 3D representation of the thresholded volume in a region of interest (Figure 24,

26-28).The changes between the three different scans can be seen even better. It also gives a better view on the damaged coco pops.

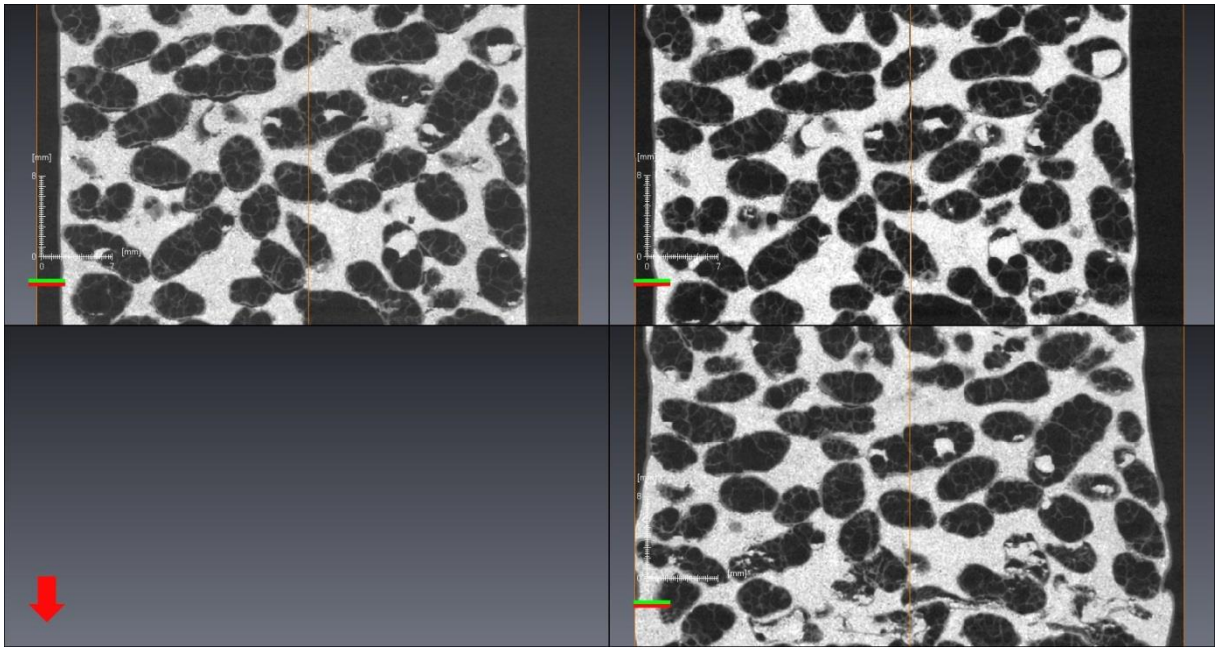

Figure 23 Images of the three scans of the sample, before the loading, at the peak stress and after loading, zoomed in.

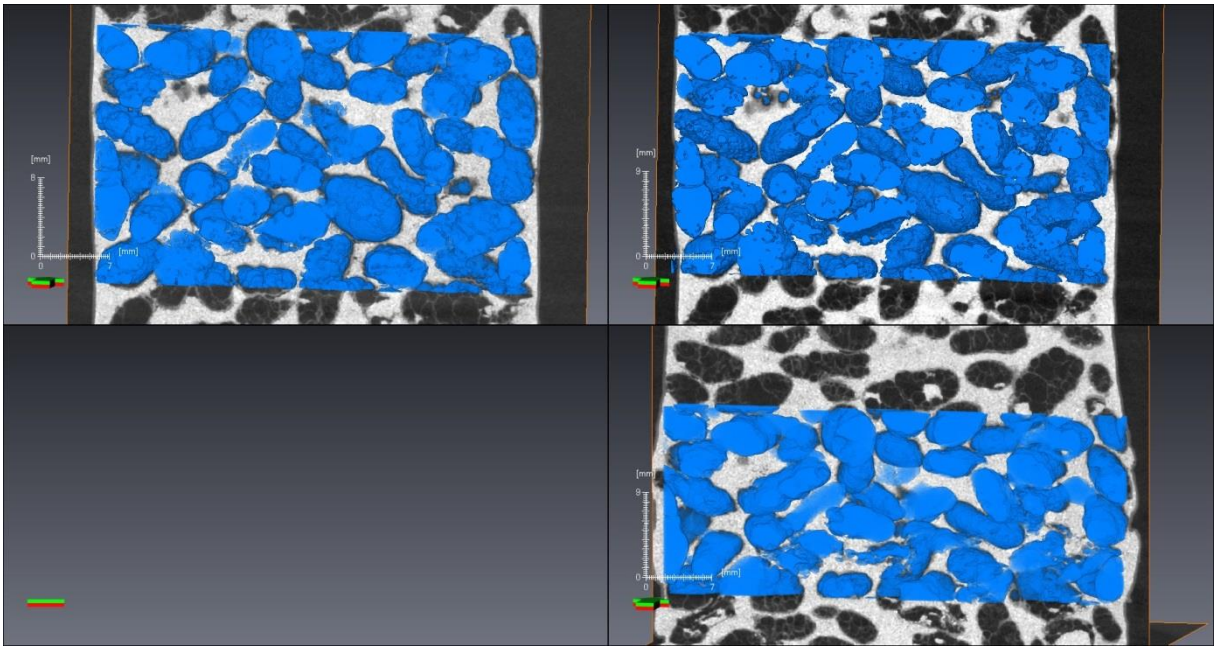

Figure 24 Visualisation of the three scans of the sample.

On the last scans crushed coco pops are flat and fragmented in several pieces. The small particles of a crushed coco pops are situated along the line at which most coco pops are broken.

When further zooming (figure 25), the process of particle crushing can be further visualised. The coco pop at the centre of the yellow box is hollow and partially filled in with sand. At peak stress, its cavity has already collapsed. This is the only particle damage that could be seen on the scans at this stage. The coco pop is further deformed at the 13% strain stage. At the vicinity of this grain, there is another hollow coco pop. It is at the centre of the red box. At peak stress this coco pop is still intact

but at the last stage of the test, it is completely flattened. The collapse of the first coco pop has caused a stress redistribution which triggered the collapse of the second hollow grain. At the vicinity of both grains, other fragmented and crushed grains can be spotted.

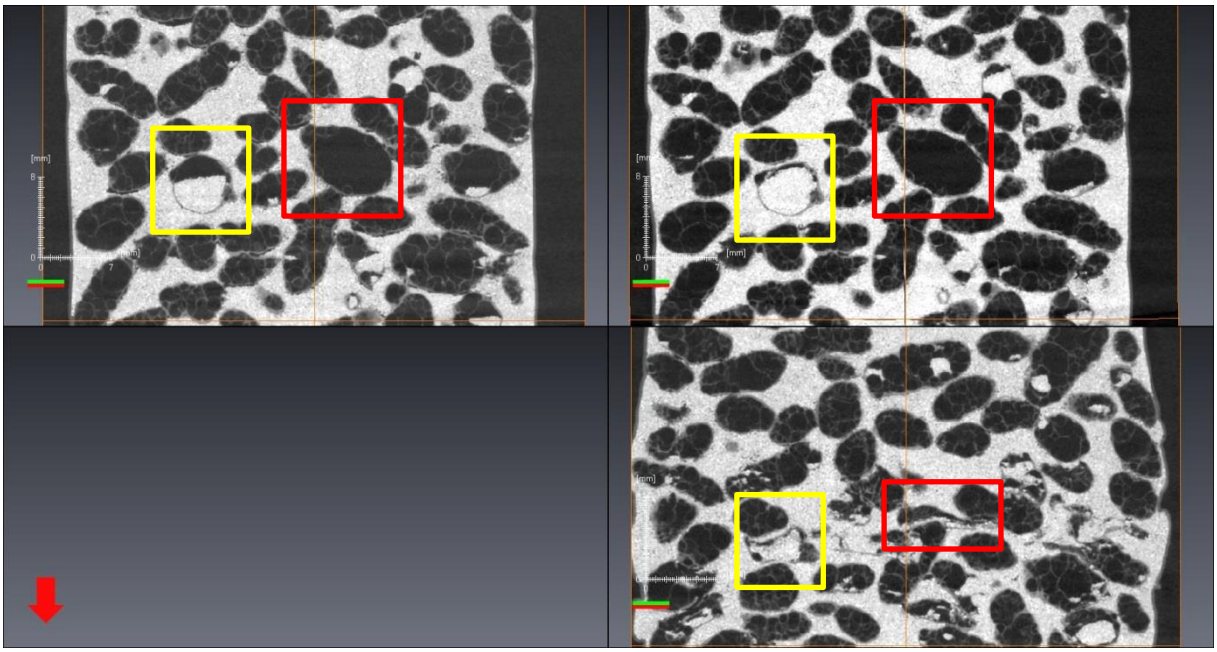

Figure 25 Image of two coco pops with voids that are filled with air (highlighted with the yellow and red squares)

By thresholding the coco pops, including their void space, from the sand and representing the thresholded volume in the region of interest, the implosion of the large cavities present in both grains is represented in 3D in Figure 26 & 27.

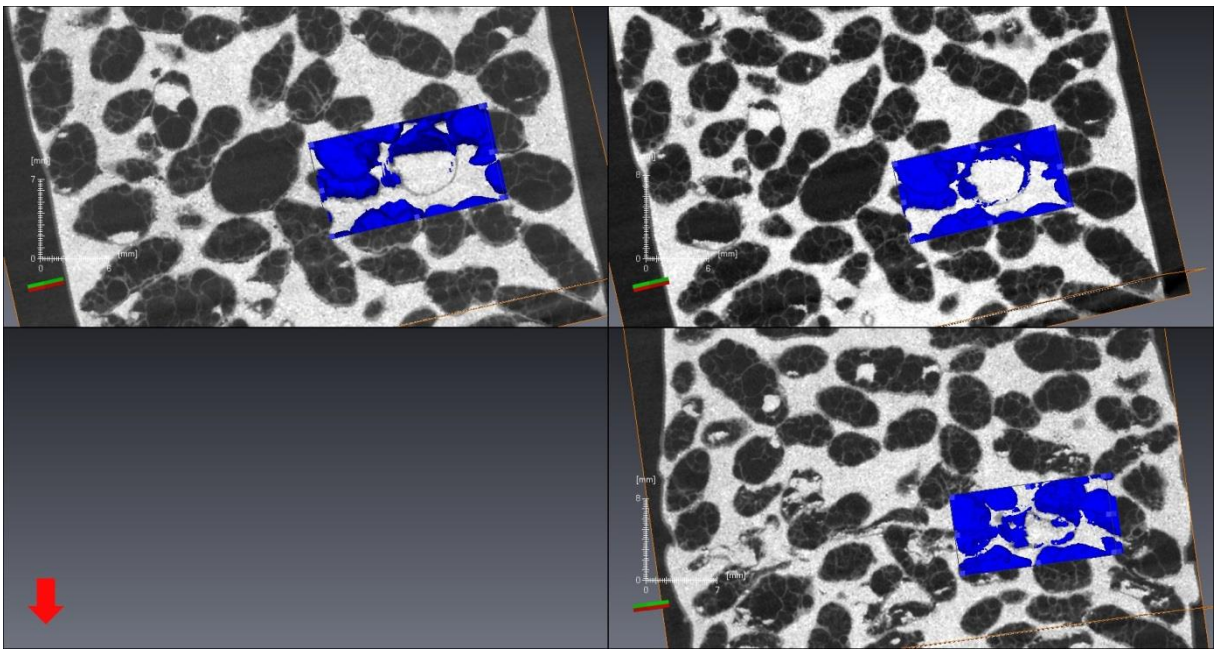

Figure 26 Visualisations of three scans of a coco pop with a void initially filled with air.

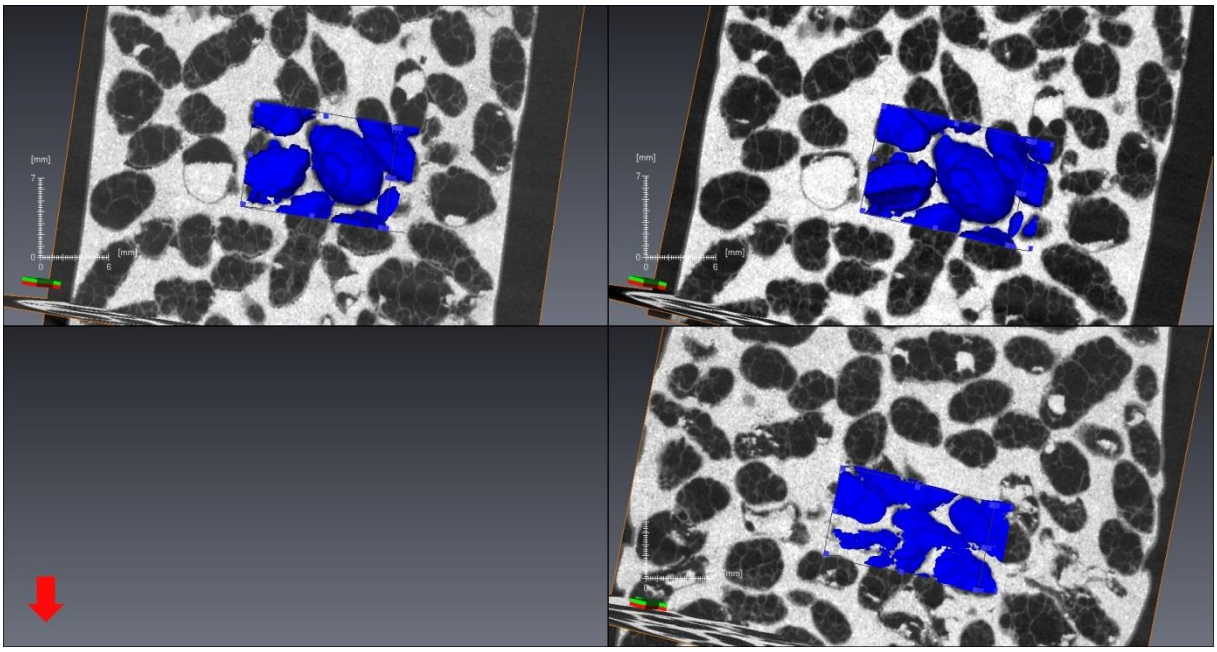

Figure 27 Visualisations of three scans of another coco pop with a void initially filled with air.

Suggestions for quantifying the displacement, rotation and crushing of the coco pops are given in the Recommendation chapter.

Quantification of the sample deformation and fraction of coco pops in sand

The volume of coco pops in the sample has also been calculated before testing and after testing (

Table 9). How this has been done and which steps were taken in Avizo Fire can be found in Appendix B.

	Before [mm^3]	After [mm^3]
Sample	109864	105234
Sand	61373	56898,42
Coco pops	48491	48335,58

Table 9 Volumes calculated using Avizo for sample 3 before and after loading

Preliminary results indicate that the sample has sustained a volumetric contraction during shearing. The fraction of coco pops in the analysed volume has slightly increased (44.13 and 45.93 %) which is not as expected from the observation of the scans since at the final stage of the test, several grains have crushed and their inner voids have collapsed and have been filled in by sand. The results of the image processing has to be double-checked.

6.4 Discussion

At the first test, the axial strain applied to the sample should have been higher to get a better idea of the strength of a layer coco pops. Now it is difficult to say if the coco pops would survive under a higher stress.

The second and third test have been executed up to larger vertical strains. The scans show that the way the coco pops have been manually distributed in the sample can definitely be better. The coco pops have not been pluviated like the sand has and the density of the coco pops may differ throughout the sample. Scanning the whole sample would allow a better comparison between the scans and between the scans and the macroscopic behaviour of the sample. It would also help to check the boundary conditions of the test .

Even if Avizo Fire can do a lot, it is not always done perfectly. The thresholded domain has to be carefully inspected before the volume estimations made in this thesis can be validated.

In theory, individual particles can be tracked using AVIZO by separating each coco pop from its neighbours and measuring a number of its morphometric parameters such as 3D volume, 3D area, orientation and length of main axes as well as location of gravity centre. In practice, separation is difficult. Due to their oblong shape, the grains are often split in two or more pieces (Figure 28). After separation, wrongly split fragments should be merged. This is possible using a specific script in AVIZO but could not be done within the framework of this BSc thesis due to the lack of time. as it would take a lot of time, and time not available for this BSc thesis.

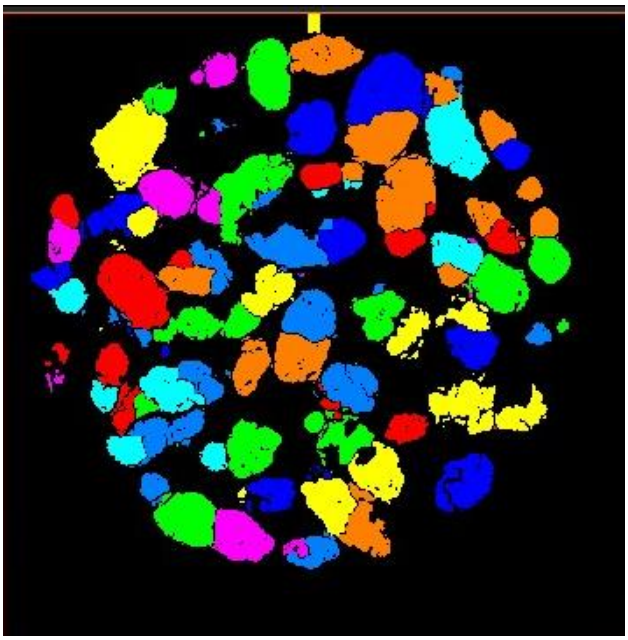

Figure 28 Label Analysis done in Avizo Fire to calculate the volume of every coco pop.

7. Conclusions

Coco pops are not really considered strong since they are crushable by hand but when embedded in sand, however, they are protected by sand and can resist to higher stresses. When coco pops are completely surrounded by sand, the chance of survival is much larger as can be seen in chapter 6.1. When the coco pops are not only surrounded by sand but also have contact with each other, they are less strong (chapter 6.2 & 6.3). Under an effective confinement of 80 kPa, after a peak stress of 290 kPa, first damage is observed. As strain increases, further damage is observed in the coco pops. The damage done to the coco pops in the sample with the second configuration is especially visible along the line at which the sample had the most radial deformation. The damage along that deformation line, is almost a 100% as can be concluded from the images in chapter 6.3. The damage at the top and the bottom of the sample is 0%. No coco pop has survived if placed along the line of the most deformation while all the coco pops placed further away from the line with the most radial deformation are without damage. The coco pops approximately two centimetres above and below this line also have a chance of getting damaged as there are located in the band where shear strain is localised.

When voids are present in a coco pop it depends on the filling of these void if the coco pops tend to get crushed. When a coco pop has an internal void filled with air, the sand cannot enter the void, the coco pop is likely to get crushed. When a coco pops void is partially filled with air and the other part already with sand, it has a higher chance of surviving the loading and it will also remain stronger. Small voids do not tend to have a lot of influence in the strength of the coco pops as long as they are filled with sand for support. According to Getrouw (2014), the charred seeds carbonized at 370^{o}C , for which the coco pops are an analogue, are twice as weak as the coco pops. That would mean more damage would be done to the charred seeds than now has been concluded for the coco pops. In order to find out, another investigation has to be done with real archaeological charred seeds.

The approach for this investigation has proved to be feasible and can definitely be used for investigating the real charred organic seeds.

The dry air pluviation method requires experience and dexterity to be produce a homogeneous sample at a given density.

The micro-CT scan is a good way to analyse the integrity of charred seeds. With the micro CT scans and the Avizo software each organic seeds can be seen accurately just as the coco pops can be seen.

8. Recommendations

In order to create accurate and precisely the same sample over and over again, a dry air pluviation machine would be really useful. This way the funnel can get raised at a constant speed and the sand can get distributed over the sample equally without any small flaws caused by a shiver of the hand. With this machine, the samples can be created more easily and faster as well.

When creating samples with charred organic seeds a method has to be found in order to distribute those equally as well. When placing two layers in a sample, it is not really necessary, but when wanting to create a reproducible sample with the entire mould filled with charred organic seeds a good method will be useful.

Vacuum is applied throughout the whole investigation of a sample (testing and scanning). In order to apply a vacuum, a pump was installed with a hose and valves to create a system which could be transported. Every time a sample was made and it had to be moved to either the universal testing machine or the micro CT-scanner, the entire system, with everything connected except for the pump to the power source, had to be moved. Two people were needed. Another way has to be found to apply vacuum, transport the sample and then apply vacuum again, in order to make it easier for one person to do the investigation.

Placing the sample in the micro CT-scanner was not the easiest thing to do as well. In order to keep vacuum on the sample the pump had to be placed inside the micro CT scanner with all the hoses and valves as well since the micro CT-scanner has to be closed in order to scan. All the hoses in the system made it difficult the place the sample the right way and the fact the sample turns around during scanning has to kept in mind as well.

The scanning of the sample itself was not always going without problems. The hose connected to the bottom plate was too stiff in order to be bent during the rotation of thee rotating platform. Therefore it sometimes stopped scanning and it had to be helped by moving the hose to the other side of the sample for example so the micro CT-scanner could turn the sample again. When the hose is connected to the bottom plate with a cornered connector, it would be easier for the micro CT-scanner to turn the sample 360°.

A scan took about 1 hour. Only part of the sample was scanned. It is recommended to scan the full sample for a better relation between macro- and microscopic behaviour.

Due to a lack of time, the scans have only been partially analysed in Avizo Fire. An analysis of the entire sample in which each coco pop or charred organic seed is tracked throughout the testing would give significantly more information of the degree of integrity of the coco pop fraction. However, a lot of time is needed as well as some good knowledge about Avizo Fire to make that work.

9. Reference List

ANARAKI, K. E. 2008. *Hypoplasticity Investigated: Parameter Determination and Numerical Simulation.* MSc, Delft University of Technology.

COUNCIL OF EUROPE 1992. European Convention on the Protection of the Archaeological Heritage (Revised). Strasbourg: Council of Europe.

GEOTECHDATA.INFO. 2010. *Triaxial Test* [Online]. Geotechdata.info. Available: http://www.geotechdata.info/geotest/triaxial-test.html [Accessed June 6th 2014].

GETROUW, N. A. S. 2014. *1-D Loading of charred particles.* BSc, Delft University of Technology.

HYDE, A. F. L., JACKSON, C.M., HASSAN, I. AND HOWIE, L.A. 2010. Probability of damage to archaeological inclusions in a sandy matrix. *In:* JIANG, M., LIU, F. AND BOLTON, M. (ed.) *Geomechanics and Geotechnics: From Micro to Macro.* CRC Press.

STUIT, H. G. 1995. *Sand in the geotechnical centrifuge.* PhD, Delft Univeristy of Technology.

VAN DER PUTTE, E. A. V. 2011. *The strength of carbonized wheat.* BSc, Delft University of Technology.

VAN DIJK, N. N. 2014. *The behaviour of artificial archaeological remains during a one-dimensional compression test.* BSc, Delft University of Technology.

VAN NES, J. H. G. 2004. *Application of computerized tomography to investigate strain fields caused by cone penetration in sand.* Msc, Delft University of Technology.

WOOD, D. M. 2008. Modelling granular materials: discontinuum - continuum. *In:* CHEN, J. F., OOI, J.Y. AND TENG, J.G. (ed.) *Structures and Granular Solids: From Scientific Principles to Engineering Application.* Edinburgh: CRC Press.

Appendix A

Falling Height (mm)	Test Number	Initial mass (g)	Final mass (g)	Sample mass (g)	Total height (mm)	Sample height (mm)	Volume (cm^3)	Density (g/cm^3)
27,67	1	1007,3	695,35	311,95		111,78	215,98	**1,444**
	2	1005,8	700,53	305,27	173,4	109,06	210,73	**1,449**
	3	1004,96	690	314,96	173,7	109,36	211,31	**1,491**
	4	1003,5	690,12	313,38	173,95	109,61	211,79	**1,480**
37,67	1	996,65	672,98	323,67	173	108,66	209,95	**1,542**
	2	995,12	680,98	314,14	173,1	108,76	210,15	**1,495**
20,67	1	994,75	690,11	304,64	171,1	106,76	206,28	**1,477**
	2	994,65	690,28	304,37	172	107,66	208,02	**1,463**
	3	994,68	688,07	306,61	173,85	109,51	211,60	**1,449**
	4	994,44	681,82	312,62	172,7	108,36	209,37	**1,493**
	5	994,01	685,81	308,2	172,1	107,76	208,21	**1,480**
30,67	1	993,8	673,06	320,74	173,55	109,21	211,02	**1,520**
	2	993,31	671,28	322,03	174,1	109,76	212,08	**1,518**
	3	992,5	680,96	311,54	174	109,66	211,89	**1,470**
	4	992,32	676,16	316,16	174,15	109,81	212,18	**1,490**
40,67	1	991,73	666,41	325,32	174,6	110,26	213,04	**1,527**
	2	991,28	670,41	320,87	173,1	108,76	210,15	**1,527**
	3	990,34	660,15	330,19	174,85	110,51	213,53	**1,546**
	4	990,14	664,74	325,4	174,9	110,56	213,62	**1,523**
	5	989,67	658,74	330,93	173,75	109,41	211,40	**1,565**
50,67	1	989,21	658,3	330,91	173,3	108,96	210,53	**1,572**
	2	988,54	653,73	334,81	174,3	109,96	212,47	**1,576**
	3	988,41	653,23	335,18	174,15	109,81	212,18	**1,580**
	4	987,73	656,09	331,64	174,65	110,31	213,14	**1,556**

Appendix B

In order to get a good estimate of the volume of the coco pops present in the sample, multiple actions have to be done in Avizo Fire.

1. First data is imported from the micro CT scanner.

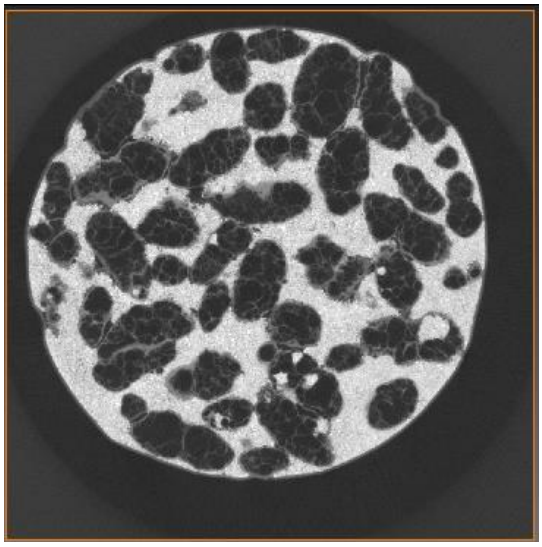

Figure 29 Top view of sample without processing

2. The volume of this dataset is edited to select the relevant part of the scan (the sample) and discard noise outside the sample. As the sample is not perfectly cylindrical, the edited volume still contains some irrelevant zones.

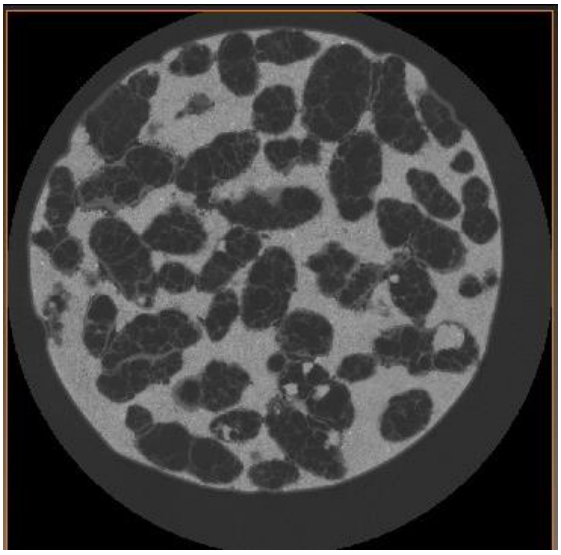

Figure 31 Top view of sample with volume edited

3. The following steps aim at selecting the sample only. This done using “interactive thresholding”. This way a part of the image is holded to use for further actions. First the sample and the densest parts of the coco pops are thresholded.

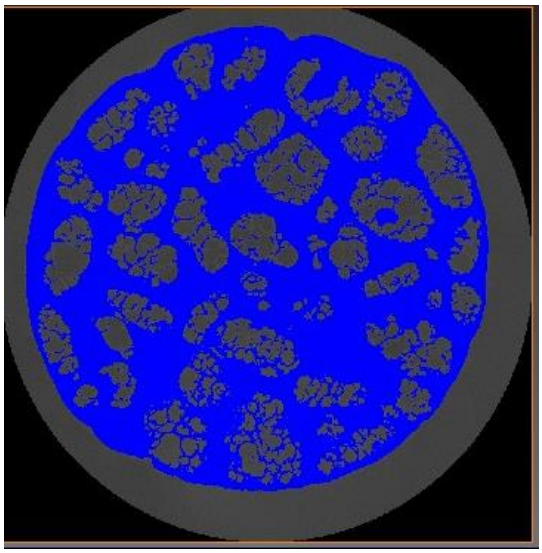

Figure 30 Thresholded image of the sample

4. Next the holes in the volume thresholded at step 3 are filled. This means that the coco pops grain that are not thresholded in step 3 are filled in order to select the entire sample.

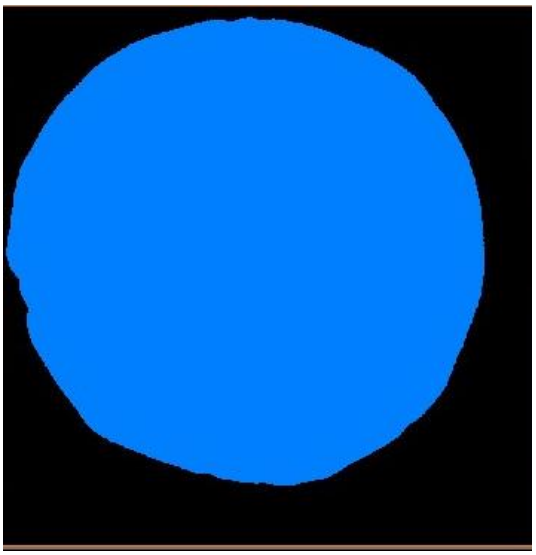

Figure 32 Thresholded image of the sample with the holes filled.

5. When processing small spots outside the region of interested get selected as well. Those have been removed before continuing.

6. The volume of the selected part of the image can be calculated by using a function called “Label Analysis”. This will calculate the volume of every individual part that is selected. Since only one selection is made, it calculates only one volume.

7. Now the volume of the entire sample (sand and coco pops) has been calculated. The volume of the sand can be calculated. The volume edited image is thresholded again but in a different way.This time, the coco pops are thresholded in the edited volume of step 1. In the thresholding process, the void fringing the sample is also thresholded.

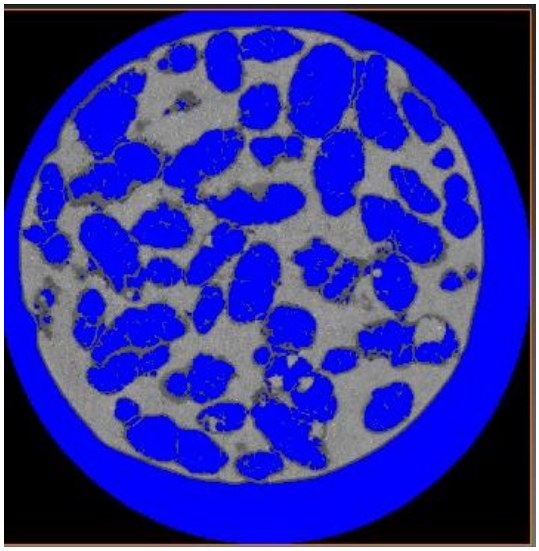

Figure 33 Image of differently thresholded sample.

8. This step is the uses the same function as in step 6 but now on the new selection.

9. The sand volume can now be calculated. First the function “Not Image” is used on the image created at step 6, which selects everything that 6. The volume of the selected part of the image can be calculated by using a function called “Label Analysis”. was not selected and the other way around.

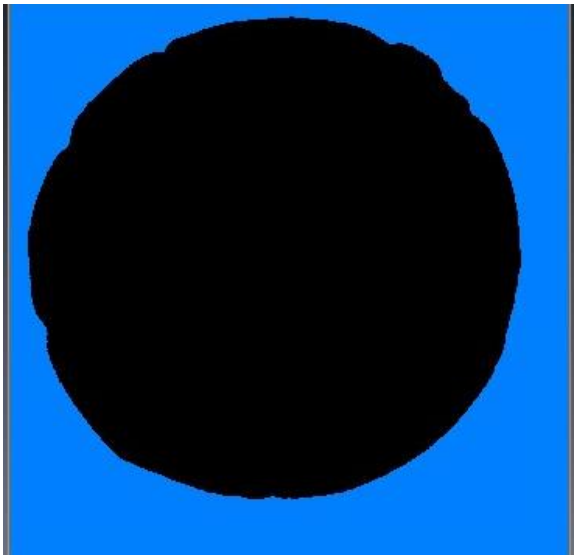

Figure 34 Image of the sample after the "Not Image" function has been used.

10. The image of the selected surroundings of the sample is now combined with the image of the coco pops and the surrounding using an “Or Image” command.

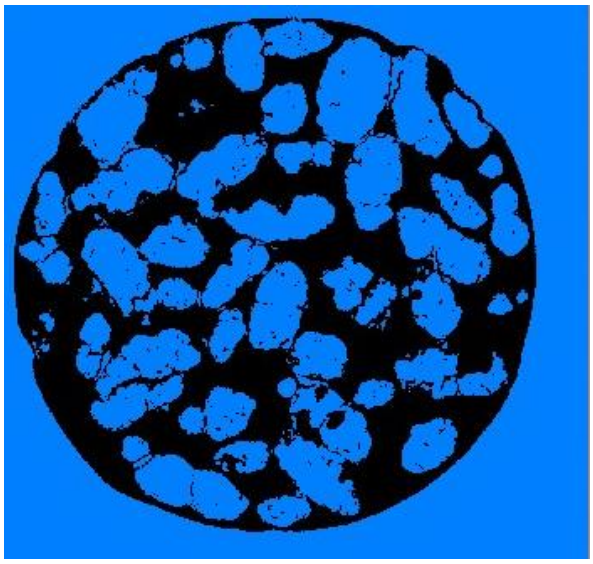

Figure 35 Combination of multiple image to select everything except the sand.

12. Again, the “Not Image” function is used which creates a selection of only sand.

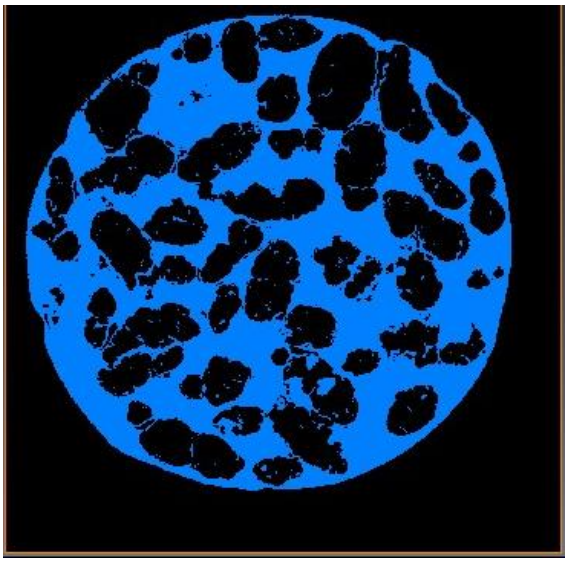

Figure 36 Only the sand in the sample is selected in this image.

12. Again a label analysis is done, which provides the volume of the sand in the sample.

13. Now the volume of the grains can be calculated by subtracting the volume of the sand from the total sample volume.